Correlations in Ultracold Trapped Few-Boson Systems: Transition from Condensation to Fermionization

Sascha Zöllner[*]

Theoretische Chemie, Institut für Physikalische Chemie,

Universität Heidelberg, INF 229, 69120 Heidelberg, Germany

Hans-Dieter Meyer[†]

Theoretische Chemie, Institut für Physikalische Chemie,

Universität Heidelberg, INF 229, 69120 Heidelberg, Germany

Peter Schmelcher[‡]

Theoretische Chemie, Institut für Physikalische Chemie,

Universität Heidelberg, INF 229, 69120 Heidelberg, Germany and

Physikalisches Institut, Universität Heidelberg,

Philosophenweg 12, 69120 Heidelberg, Germany

Abstract

We study the correlation properties of the ground states of few ultracold bosons, trapped in double wells of varying barrier height in one dimension. Extending previous results on the signature of the transition from a Bose-condensed state via fragmentation to the hard-core limit, we provide a deeper understanding of that transition by relating it to the loss of coherence in the one-body density matrix and to the emerging long-range tail in the momentum spectrum. These are accounted for in detail by discussing the natural orbitals and their occupations. Our discussion is complemented by an analysis of the two-body correlation function.

---

[*]Electronic address: sascha.zoellner@pci.uni-heidelberg.de

[†]Electronic address: hans-dieter.meyer@pci.uni-heidelberg.de

[‡]Electronic address: peter.schmelcher@pci.uni-heidelberg.de

1

I. INTRODUCTION

For more than a decade, trapped ultracold atoms have been a vastly expanding field of research [1, 2, 3, 4]. Their low thermal fluctuations, and the fact that one can virtually design both the external as well as the inter-particle forces via electromagnetic fields, make them an ideal simulation tool for various phenomena, ranging from condensed-matter physics to quantum information. A particularly intriguing aspect has been the system's dimensionality. For example, if its transverse degrees of freedom are frozen out such that an effective one-dimensional description becomes possible, then the effective interaction strength of the system may be tuned at will from a weakly correlated to a strongly interacting one by merely changing the lengthscale of the transverse confinement [5]. In the case of infinite repulsion—the so-called Tonks-Girardeau gas—the system may even be mapped to that of an ideal Fermi gas [6] and exhibits striking features, including the reduction of off-diagonal long-range order [7] or a very distinctive momentum spectrum [8]. This has also been verified experimentally [9, 10].

However, the Tonks-Girardeau limit requires low densities and is thus amenable only for *few* atoms, typically $N \sim 10 - 100$. Besides that, there is the factor of computational accessibility—which includes the fact that a small number of atoms greatly facilitates the intuitive understanding of the mechanisms underlying the physics of *large* systems. But there is yet another argument for considering few-atom systems: They permit a much higher level of control. There is no thermal cloud, as for large N, associated with decoherence and energetically dense excitations, but a pure quantum system.

However, the same reasons that make few atoms so interesting also render their solution computationally cumbersome. There have been some detailed analyses of the Tonks-Girardeau limit in a harmonic trap [11, 12], which is greatly simplified since the solution is semi-analytic. Needless to say, the complementary borderline case of weakly interacting bosons is also well understood: in this limit, the Gross-Pitaevskii equation becomes valid, which assumes that all particles condense into a single one-particle orbital (see, e.g., [1]). Comparatively little is known about the *transition* between these extremes, though. Many key features are nicely illustrated on the analytic solution of two bosons in a harmonic trap [13] or other simple models [14, 15]. Based on a multi-orbital mean-field approach valid for arbitrary traps, it has recently been demonstrated that there exists an intriguing pathway for the above transition [16]. While that ansatz captures the essential features of that evolution, it is desirable to investigate it from a rigorous many-body perspective, but still

irrespective of the trap geometry. Most of the studies so far have relied on the assumption of only few contributing orbitals [17, 18], while a recent exact diagonalization has focused on a simple harmonic trap [19]. For the case of a double-well trap, the authors have previously investigated the ground state of few interacting bosons in the entire regime between the Gross-Pitaevskii limit and fermionization for different well depths, but chiefly from the perspective of the density profiles [20].

The aim of this paper now is to address the role of correlations in these systems, in particular the relation of the fragmentation mechanism to the concept of long-range order and the momentum density. This way we not only bridge the gap between the two borderline regimes of zero and infinite repulsion but also extend our previous study. Our approach is based on the Multi-Configuration Time-Dependent Hartree method [21, 22, 23], which we use to study the numerically exact ground state of few bosons.

This article is organized as follows. In Sec. II, the model is introduced and some key quantities for the description of correlations are discussed. Section III contains a concise introduction to the computational method and how it can be applied to our problem. In the subsequent section the one-body correlation aspects are studied. More concretely, we present the full one-body density matrix in the context of long-range order in Sec. IV A, which is subsequently explained in terms of its eigenvectors and their populations (IV B). Their connection to the momentum density will then be clarified in Sec. IV C. We complement our investigation by going beyond the one-particle picture in looking at the two-body correlations in Sec. V, which is rounded off by relating our results to some common approximation schemes, the two-mode model [24] and the multi-orbital mean field.

II.   THEORETICAL BACKGROUND

A.   The model

In this article we investigate a system of *few* interacting bosons ($N = 2, \ldots, 6$) in an external trap. These particles, representing atoms with mass M, are taken to be one-dimensional (1D). More precisely, after integrating out the transverse degrees of freedom and rescaling we arrive at

the model Hamiltonian (see [20] for details)

$$H = \sum_i h_i + \sum_{i<j} V(x_i - x_j),$$

where $h = \frac{1}{2}p^2 + U(x)$ is the one-particle Hamiltonian with a trapping potential U, while V is the two-particle interaction potential with low-energy scattering length a_0, taken to be the effective interaction [5]

$$V(x) = g\delta_\sigma(x), \text{ with } g = \frac{4a_0}{a_\perp^2} \left(1 - |\zeta \left(\tfrac{1}{2} \right)| \frac{a_0}{a_\perp} \right)^{-1}.$$

Here a harmonic transverse trap potential with oscillator length $a_\perp$ was assumed. Moreover, the well-known numerical difficulties due to the spurious short-range behavior of the delta-function potential $\delta(x)$ are alleviated by mollifying it with the normalized Gaussian

$$\delta_\sigma(x) = \frac{1}{\sqrt{2\pi}\sigma} e^{-x^2/2\sigma^2},$$

which tends to δ as $\sigma \to 0$ in the distribution sense. We choose a fixed value $\sigma = .05$ as a trade-off between smoothness and a short range.

B. Fragmentation: key aspects

Although our approach equips us with the full solution of the system—here, the ground-state wave function—this solution obviously still needs to be related to the concrete physical questions. Penrose and Onsager suggested a criterion connected with the one-body density matrix, which will be laid in what follows.

As is well-known, the knowledge of the wave function Ψ is equivalent to that of the density matrix $\rho_N = |\Psi\rangle\langle\Psi|$. To the extent that we study at most two-body correlations, it already suffices to consider the two-particle density operator

$$\rho_2 = \text{tr}_{3..N} |\Psi\rangle\langle\Psi|, \tag{1}$$

whose diagonal kernel $\rho_2(x_1, x_2)$ gives the probability density for finding one particle located at x_1 and any second one at x_2. For any 1-particle operator, of course, it would be enough to know the one-particle density matrix $\rho_1 = \text{tr}_2 \rho_2$, so that the exact ground-state energy may be written as

$$E = N \, \text{tr}(\rho_1 h) + \frac{N(N-1)}{2} \text{tr}(\rho_2 V).$$

Consider the spectral decomposition of the one-particle density matrix

$$\rho_1 \equiv \sum_a n_a |\phi_a\rangle\langle\phi_a|, \tag{2}$$

where $n_a \in [0,1]$ is said to be the population of the *natural orbital* ϕ_a. If all $n'_a \equiv n_a N \in \mathbb{N}$ ($\sum_a n'_a = N$), then the density may be mapped to the (non-interacting) number state $|n'_0, n'_1, \dots\rangle$ based on the one-particle basis $\{\phi_a\}$; for non-integer values it extends that concept. In particular, the highest such occupation, n_0, may serve as a measure of *non*-fragmentation, a criterion put forward by Penrose and Onsager [25]. For $n_0 = 1$, a simple condensate is recovered. This is the well-known borderline case of the Gross-Pitaevskii eq.: as $g \to 0$, $\rho_1 \to |\phi_0\rangle\langle\phi_0|$ [26] and $\rho_2 = \rho_1 \otimes \rho_1$, so that the interaction above can be replaced by a mean field $\bar{V} = \mathrm{tr}(\rho_1 V)$.

The 1-particle density matrix may be viewed not only from the perspective of its spectral decomposition, but also in terms of its integral kernel $\rho_1(x, x') \equiv \langle x|\rho_1|x'\rangle = \rho_1(x', x)^*$. Since the density matrix is non-negative, so is the 1-particle density $\rho(x) \equiv \rho_1(x, x)$. As opposed to that, the off-diagonal part will be complex in general (though in this paper a real representation is employed). It is therefore certainly not an observable in its own right. Nonetheless, it is of some interest as it gives us access to all one-particle quantities, also non-local ones such as the momentum density $\tilde{\rho}(k) = 2\pi\langle k|\rho_1|k\rangle = \sum_a n_a|\hat{\phi}_a(k)|^2$, which can be related to the density matrix via

$$\tilde{\rho}(k) = \int dx \int dx' e^{-ik(x-x')} \rho_1(x, x').$$

It is reflection symmetric if ρ_1 is real symmetric. Moreover, it can be understood as the Fourier transform of the integrated 'off-diagonal' correlation function [1]

$$\tilde{\rho}(k) = \int dr\, e^{-ikr} \gamma(r),$$

with $\gamma(r) := \int dR\, \rho_1(R + \frac{r}{2}, R - \frac{r}{2})$. Note that γ is again generally complex and reflection symmetric, while $\gamma(0) = 1$. From this, it becomes clear that the off-diagonal behavior encoded in γ has a 1-1 correspondence to the momentum distribution. More specifically, the short-distance behavior determines the high-k asymptotics, which for a delta-type interaction $V(x) = g\delta(x)$ in the limit $g \to \infty$ has been shown to display the universal decay $\tilde{\rho}(k) = O(k^{-4})$ [8]. Conversely, the off-diagonal asymptotics $r \to \infty$ relates to the low-k regime. This, however, depends on the nature of the external potential. For a translationally invariant system, it has been argued that Bose condensation were equivalent to *off-diagonal long-range order*, i.e. $\gamma(r) = O(1)$ [27]. In the same

context, but in the limit $g \to \infty$, it has in turn been shown that $\gamma(r) = O(r^{-1/2})$, which implies an infrared divergence $\tilde{\rho}(k) \sim c/\sqrt{k}$ as $k \to 0$ [7].

The above limit $g \to \infty$ is commonly referred to as the *Tonks-Girardeau* limit of 1D hard-core bosons, or also as their *fermionization*. This lingo finds its justification in the *Bose-Fermi map* [6, 28] that establishes an isomorphy between the exact *bosonic* wave function Ψ_∞^+ and that of a (spin-polarized) non-interacting *fermionic* solution Ψ_0^-,

$$\Psi_\infty^+ = A\Psi_0^-,$$

where $A(Q) = \prod_{i<j} \text{sgn}(x_i - x_j)$ and $Q \equiv (x_1, \ldots, x_N)^T$. In particular, the ground state reduces simply to the absolute value of Ψ_0^-, which makes it tempting to think of the hard-core interaction $g \to \infty$ as mimicking the exclusion principle. As the free fermionic solution is easily accessible, this theorem has proven very fruitful in a wide range of applications. For our purposes, the most relevant one is the solution of N bosons in a harmonic trap [11]

$$\Psi_\infty^+(Q) \propto e^{-|Q|^2/2} \prod_{1 \le i < j \le N} |x_i - x_j|,$$

which illustrates the characteristic short-distance correlations.

III. COMPUTATIONAL METHOD

Our goal is to investigate the ground state of the system introduced in Sec. II for all relevant interaction strengths in a numerically *exact, i.e.,* controllable fashion. This is a highly challenging and time-consuming task, and only few such studies on ultracold atoms exist even for model systems (see, e.g., [17, 18, 19]). Our approach relies on the Multi-Configuration Time-Dependent Hartree (MCTDH) method [21, 23, 29], primarily a wave-packet dynamics tool known for its outstanding efficiency in high-dimensional applications. To be self-contained, we will provide a concise introduction to this method and how it can be adapted to our purposes.

The underlying idea of MCTDH is to solve the time-dependent Schrödinger equation

$$\begin{cases} i\dot{\Psi} = H\Psi \\ \Psi(Q, 0) = \Psi_0(Q) \end{cases} \tag{3}$$

as an initial-value problem by expansion in terms of direct (or Hartree) products Φ_J:

$$\Psi(Q, t) = \sum_J A_J(t) \Phi_J(Q, t) \equiv \sum_{j_1=1}^{n_1} \cdots \sum_{j_f=1}^{n_f} A_{j_1 \ldots j_f}(t) \prod_{\kappa=1}^{f} \varphi_{j_\kappa}^{(\kappa)}(x_\kappa, t), \tag{4}$$

using a convenient multi-index notation for the configurations, $J = (j_1 \ldots j_f)$, where f denotes the number of degrees of freedom and $Q \equiv (x_1, \ldots, x_f)^T$. The (unknown) *single-particle functions* $\varphi_{j_\kappa}^{(\kappa)}$ are in turn represented in a fixed, primitive basis implemented on a grid. For indistinguishable particles as in our case, the sets of single-particle functions for each degree $\kappa = 1, \ldots, N$ are of course identical (i.e., we have φ_{j_κ}, with $j_\kappa \leq n$).

Note that in the above expansion, not only the coefficients A_J are time-dependent, but so are the Hartree products Φ_J. Using the Dirac-Frenkel variational principle, one can derive equations of motion for both A_J, Φ_J [23]. Integrating this differential-equation system allows one to obtain the time evolution of the system via (4). Let us emphasize that the conceptual complication above offers an enormous advantage: the basis $\{\Phi_J(\cdot, t)\}$ is variationally optimal at each time t. Thus it can be kept fairly small, rendering the procedure very efficient.

It goes without saying that the basis vectors Φ_J are not permutation symmetric, as would be an obvious demand when dealing with bosons. However, the symmetry can be enforced on Ψ by symmetrizing the coefficients A_J, even though this turns out to be unnecessary as long as identical single-particle functions are employed.

The Heidelberg MCTDH package [30], which we use, incorporates a significant extension to the basic concept outlined so far. The so-called *relaxation method* [31] provides a way to not only *propagate* a wave packet, but also to obtain the lowest *eigenstates* of the system. The underlying idea is to propagate some wave function Ψ_0 by the non-unitary $e^{-H\tau}$ (*propagation in imaginary time*.) As $\tau \to \infty$, this automatically damps out any contribution but that stemming from the true ground state $|J = \mathbf{0}\rangle$,

$$e^{-H\tau}\Psi_0 = \sum_J e^{-E_J\tau}|J\rangle\langle J|\Psi_0\rangle.$$

In practice, one relies on a more sophisticated scheme termed *improved relaxation*. Here $\langle\Psi|H - E|\Psi\rangle$ is minimized with respect to both the coefficients A_J and the configurations Φ_J. The equations of motion thus obtained are then solved iteratively by first solving for A_J (by diagonalization of $(\langle\Phi_J|H|\Phi_K\rangle)$ with fixed Φ_J) and then propagating Φ_J in imaginary time over a short period. That cycle will then be repeated. The improved-relaxation method is outlined in Ref. [21]; a more comprehensive account is also available [32].

As it stands, the effort of this method scales exponentially with the number of degrees of freedom, n^N. This restricts our analysis in the current setup to about $N = O(10)$, depending on how decisive correlation effects are. If these are indeed essential, it has been demonstrated [20] that at
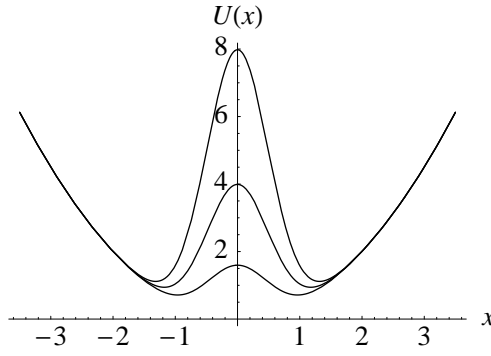
Figure 1: Sketch of the model potential $U(x) = \frac{1}{2}x^2 + h\delta_w(x)$, consisting of a harmonic trap plus a normalized Gaussian of width $w = 0.5$ and barrier strengths $h = 2, 5, 10$.

least $n = N$ orbitals are needed for *qualitative* convergence alone, while the true behavior may necessitate many more. As an illustration, we consider systems with $N \sim 5$ and use $n \sim 15$ orbitals. By contrast, the dependence on the primitive basis, and thus on the grid points, is not as severe. In our case, the grid spacing should of course be small enough to sample the interaction potential. We consider a discrete variable representation [33] of 95 harmonic-oscillator functions, which is equivalent to 95 grid points.

IV. ONE-BODY CORRELATIONS

As in Ref. [20], we consider the ground-state properties of bosons in a double-well trap modeled by

$$U(x) = \frac{1}{2}x^2 + h\delta_w(x).$$

This potential is a superposition of a harmonic oscillator (HO), which it equals asymptotically, and a central barrier which splits the trap into two fragments (Fig. 1). The barrier is shaped as a normalized Gaussian δ_w of width $w = 0.5$ and 'barrier strength' h.

For $h = 0$, the case of interacting bosons in a harmonic trap is reproduced. In Ref. [20], we have described the transition from a simple, weakly interacting condensate ($g \to 0$) to fragmentation and finally the *Tonks-Girardeau* limit ($g \to \infty$). As $h \to \infty$, the energy barrier will greatly exceed the energy available to the atoms, and we end up with two *isolated wells*. A larger g then affects only the fragmentation *within* each of these wells. In between, there is an interesting interplay between the 'static' barrier (h) and 'dynamical barriers' in the form of inter-particle forces (g),
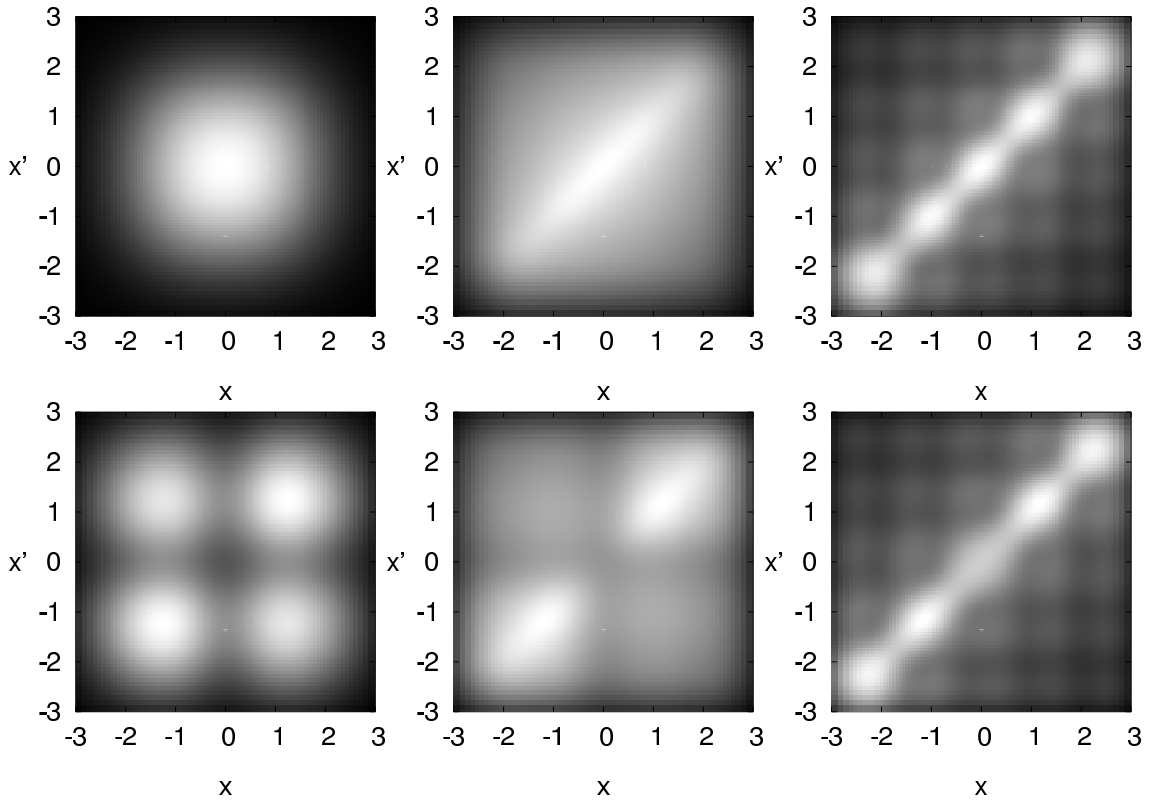
Figure 2: 1-particle density matrix $\rho_1(x, x')$ for $N = 5$ bosons. Top row: harmonic trap, bottom row: double well (barrier height $h = 5$). Results are shown for the interaction strengths $g = 0.4,\ 4.7,\ 194$ from left to right.

which has been analyzed mainly from the viewpoint of spatial *densities*.

We now seek to extend that investigation to non-local properties, such as the off-diagonal density matrix (Sec. IV A) and the momentum density (IV C), so as to attain a deeper insight into the nature of the above transition. The role played by correlations will also be highlighted by showing how *all* the natural populations evolve as a function of g.

A.   One-particle density matrix and long-range order

The 1-particle density matrix ρ_1 contains all the information about the one-particle aspects of the system, and serves as a good measure for the degree of fragmentation. In this section, we will analyze it from the most immediate perspective, i.e., we investigate its integral kernel $\rho_1(x, x')$. Although it is not an observable in itself, being generally complex-valued, it is indirectly accessible e.g. via interferometry experiments [1]. More importantly, the density matrix relates to salient

questions such as off-diagonal long-range order or the momentum distribution (see II B). Insofar it serves as a good starting point for our discussion of fragmentation in double-well systems.

In Figure 2, the fragmentation transition as reflected in $\rho_1(x, x')$ is visualized for $N = 5$ bosons in a harmonic trap ($h = 0$, top row) and a double well of barrier strength $h = 5$ (bottom). In the harmonic case, the system starts at $g = 0$ with a direct-product state $\psi = \phi_0^{\otimes N}$, i.e., with a density matrix $\rho_1(x, x') = \phi_0(x)\phi_0^*(x') \propto e^{-R^2}e^{-r^2/4}$ in terms of $r = x - x'$ and $2R = x + x'$. From this point of view, the system does not exhibit off-diagonal long-range order, which is simply rooted in the fact that it is spatially bounded. Of course, it is nonetheless in a coherent state and thus features *weak* long-range order in that $\rho_1(x, -x) \sim \sqrt{\rho(x)\rho(-x)}$ as $x \to \infty$. This property persists so long as the correlations induced by the interactions are weak enough for the system to remain in such a single-particle state (the Gross-Pitaevskii regime), such as for $g = 0.4$. For $g = 4.7$, however, the symmetry in R and r breaks up. The density profile $\rho(x) \equiv \rho_1(x, x)$ flattens, and one can see that the off-diagonal range is somewhat extended, too. However, as g is increased further, the support of $\rho_1(x, x')$ will concentrate more and more in the central region $\{x = x'\}$, where the typical fermionized profile is recovered (cf. $g = 194$). By contrast, the off-diagonal contributions will be washed out, indicating the decoherence of the system. Still it is noteworthy that even in this limit, a rest of coherence is preserved in a faint checkerboard pattern.

For the double well ($h = 5$; bottom row), the situation is apparently different. As always, the system exhibits coherence to begin with (cf. $g = 0.4$), only that the orbital is now delocalized in both minima $\pm x_0$ and may be written as $\phi_0(x) = c[\varphi(x - x_0) + \varphi(x + x_0)]$. Unlike the harmonic case, the off-diagonal range is not initially increased but directly destroyed upon switching on g. While for $g = 4.7$, the density matrix $\rho_1(x, x')$ may still be thought of as pertaining to two separate subsystems, it eventually reaches the Tonks-Girardeau limit ($g = 194$), where the only essential difference toward $h = 0$ consists in the density suppression at $x, x' = 0$.

B. Natural orbitals and their populations

While, in principle, the *full* density matrix $\rho_1(x, x')$ as studied in the previous section contains all the information about fragmentation at the one-particle level, it is somewhat less amenable to intuition. A handier criterion is offered by its spectral decomposition (2) in terms of its *natural orbitals* ϕ_a and their populations n_a, telling us how close the system is to a pure one-orbital state.
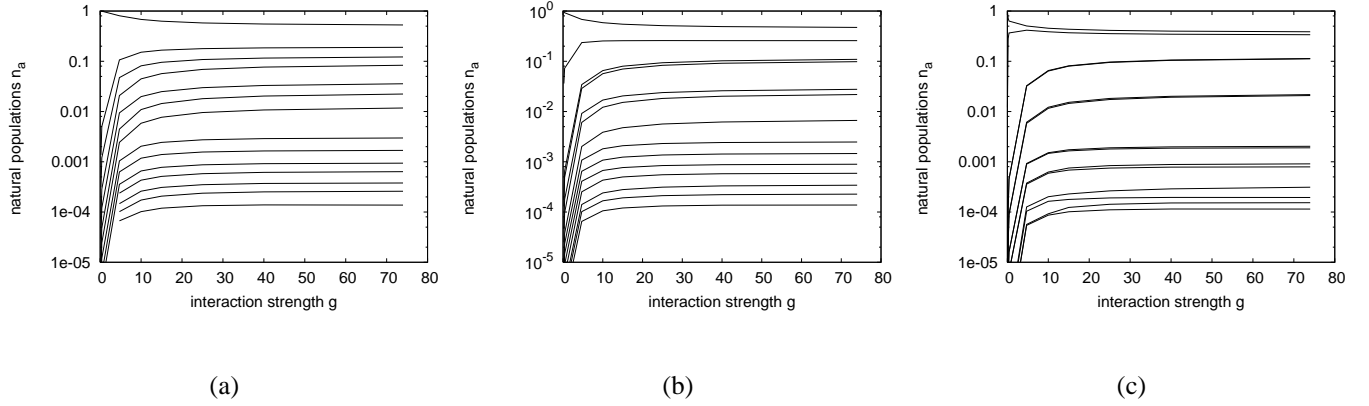
10

Figure 3: Natural populations $n_a(g)$ ($a \leq 13$) for $N = 4$ bosons in a harmonic trap (a) and in a double well with barrier height $h = 5$ (b) , $h = 10$ (c).

1. *Natural populations as a measure of fragmentation*

Figures 3(a-c) show typical plots of the natural populations as the interaction is increased, $\{n_a(g)\}$, for four bosons and $h \in \{0, 5, 10\}$. Starting from $n_0 = 1$ for the non-interacting case, the lower lines rise steeply until they end up saturating in a fermionized state at $g \to \infty$. Note that this pattern is to some degree universal. In other words, it is roughly detached from the specific shape of the trap, i.e, from what the underlying *orbitals* look like. This indicates why the set $\{n_a\}$ lends itself as a handy criterion for fragmentation. The details of the system are essentially encoded in (i) the exact sequence of n_a in the Tonks-Girardeau limit, and (ii) in the transition between the two extreme regimes $g = 0$ and $g \to \infty$.

For the harmonic oscillator ($h = 0$), the plot reveals a relatively simple hierarchy. The value of n_0 decreases smoothly to its Tonks-Girardeau limit $N^{-0.41}$ [11]. All the remaining populations increase dramatically up until $g \sim 10$, and accumulate in a more or less equidistant spacing (on a log scale). But even the next-to-dominant weight n_1 is nowhere near the 'condensate' fraction n_0; the obvious gap between these two reflects the difficulty to observe fragmentation in the harmonic oscillator as compared to $h > 0$. Note that the group of lines $\{n_0, \ldots, n_{N-1}\}$ reveals a discernible separation from the lines below. This clearly relates to the finding that the convergence of the energy $E(n)$ as a function of the number of orbitals, just to give an example, gets strikingly better once $n \geq N$ [18, 20]. It is the accumulation of points $n_a(g)$ that makes for the utter slowness of *true* convergence pointed out in that work.

For a barrier with height $h = 5$, a little more structure can be identified in the line sequence $n_a(g)$. The accumulation persists, but at least the more populated orbitals a seem to come in groups of two. This will become clearer when looking into the natural orbitals. Even more striking is the behavior of the second orbital's population, n_1. It increases with g much more rapidly than all others, and it becomes comparable with n_0 already for modest $g \sim 5$. This scale separation between the pair $n_{0/1}$ and the rest is in sharp contrast to the HO case. It gives a qualitative justification of the two-mode approximation widely used in double-well systems. To make these points even clearer, we have plotted the results for a much higher barrier, $h = 10$. Here n_1 'jumps' almost instantaneously ($g \ll 1$) to a value of order $\frac{1}{2}$, whereas the remaining occupations only catch up for $g \sim 5$. It is in that regime that the 2-mode model works brilliantly (see also Sec. V B).

The reason why fragmentation is facilitated when the central barrier is raised is intuitively clear. The particles' tendency to separate due to repulsion is usually obstructed by the higher costs of kinetic and potential energy. The potential-energy barrier creates an additional incentive for the bosons to separate. This has also been argued on more quantitative grounds (see, e.g., [24]). In a naive single-particle picture, the energy gap Δ in a double well between anti- and symmetric state, $\phi_{\pm}(x) = c[\varphi(x - x_0) \pm \varphi(x + x_0)]$, vanishes as $h \to \infty$. It is thus far easier for the interaction to bridge that gap for larger barriers, in particular compared to the gap for $h = 0$, $\Delta = 1$.

Our final remark concerns the dependence on the atom number N. For odd N, two features of the even-N picture will differ. First, the second mode is less relevant (e.g. for $N = 5$, $n_1|_{g=4.7} = 0.16$). What is more, the separation between the first N populations and all others was found to be much smaller. This backs up the intuitive notion that, for odd N, fragmentation is seemingly impeded [20].

2. Natural orbitals

Even though the natural orbitals (ϕ_a) are not of direct physical importance, they are a valuable tool to gain some insight into the process of fragmentation, as they determine both the spatial density matrix $\rho_1(x, x')$ as well as the momentum density $\tilde{\rho}$, to be discussed in the following subsection. In the uncorrelated case $g = 0$, the system is in a number state $|N, 0, \dots\rangle$ and thus the natural orbitals coincide with the single-particle eigenstates. Since V is a continuous perturbation, the orbitals ϕ_a will be somewhat distorted in the course of increasing g. For small enough g—i.e., in the Gross-Pitaevskii regime—that modified ϕ_0 will suffice for an accurate description. Con-
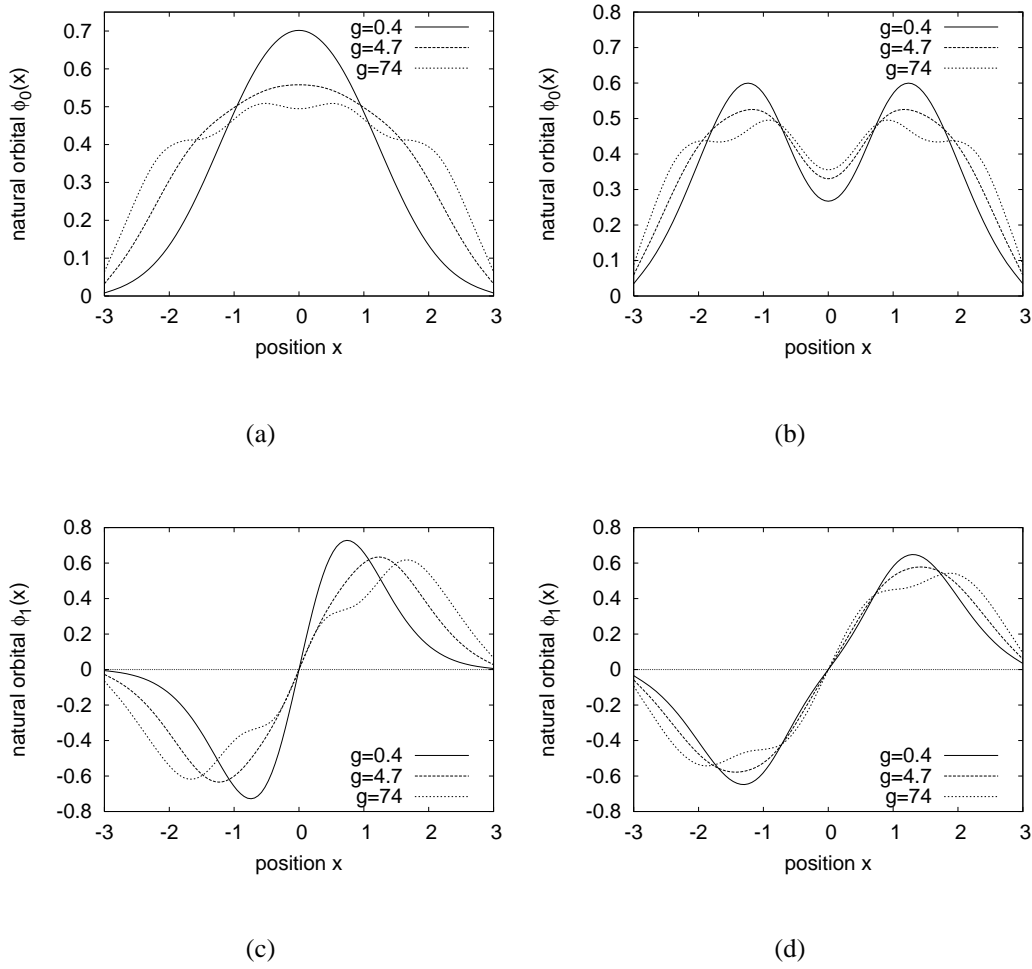
(a)

(b)

(c)

(d)

Figure 4: Natural orbitals ϕ_a for the case $N = 4$. Top row: 'condensate' orbital ϕ_0 for $h = 0$ (a), $h = 5$ (b). Bottom: ϕ_1 for $h = 0$ (c), $h = 5$ (d). Each subfigure shows plots for the representative interaction strengths $g = 0.4$ (weak repulsion), $g = 4.7$ (intermediate regime), and $g = 74$ (fermionization limit).

versely, if correlations are sufficiently influential, many orbitals will contribute to ρ_1, and studying their interplay will illuminate our results on the density matrix and the momentum distribution.

Harmonic trap ($h = 0$) For the harmonic trap (Figs. 4a,c), the initial HO function ϕ_0 is only slightly flattened in the Gross-Pitaevskii regime (cf. $g = 0.4$). The onset of fragmentation not only smears out the lowest orbital, but also admixes an antisymmetric HO-type orbital ϕ_1. In the fermionization limit, it is astonishing that already ϕ_0 exhibits all the features of the fermionized density profile $\rho(x)$, that is, N pronounced humps mirroring the spatial isolation of the atoms. This is intelligible given that ϕ_0 still has a *dominant* weight, which ought to be contrasted with the philosophy of multi-orbital mean-field schemes (see, e.g., Ref. [16]), where that pattern is

produced by N spatially localized orbitals of *equal* population. That issue will be discussed in more detail in Sec. V B.

Interesting as the orbitals may be in their own right, they also prove helpful in clarifying the decoherence found in Sec. IV A. The onset of fragmentation, as for $g = 4.7$, leads to a broadened diagonal profile $\rho_1(x, x)$, but not equally so for the off-diagonal part. That is simply because the ϕ_a have alternate parity $(-1)^a$, and thus the admixture of another orbital leads to $\rho_1(x, -x) = \sum_a (-1)^a n_a |\phi_a(x)|^2$. Hence the fragmentation into different orbitals tends to deplete the off-diagonal as compared to the diagonal density. For $g = 4.7$, this effect is still tiny as $n_1 \sim 0.1$ only, and therefore outweighed by the altogether extended support of ϕ_0. However, as more and more orbitals are mixed, as is the case in the fermionization limit (see $g = 74$), this *decoherence* attains its full impact. We remark that the faint checkerboard pattern (Fig. 2) is still rooted in the dominance of the lowest orbital, $n_0 \simeq N^{-0.41}$.

Double well ($h = 5$) In the case of a central barrier (Figs. 4b,d), the natural orbitals in the non-interacting limit will again be the single-particle eigenstates, approximately the symmetric and anti-symmetric states $\phi_\pm$. In the Gross-Pitaevskii regime ($g = 0.4$), the lowest orbital is only marginally flattened due to interactions, but a tiny reduction of the off-diagonal peaks $\rho_1(\pm x_0, \mp x_0)$ hints already at a minor admixture of the antisymmetric ϕ_1. For $g = 4.7$, fragmentation has set in, not only smearing out the orbitals $\phi_{0/1}$ —and thus the diagonal profile—but along the way washing out the off-diagonal long-range order almost completely. As emphasized before, the fermionization pattern tends to be generic for different h, which reflects both in the density matrix as well as in the natural orbitals.

C. Momentum density

The discussion so far focused on rather abstract aspects of the one-body correlations. Yet it can help us cast a light on an experimentally more amenable quantity, the momentum density.

Harmonic trap ($h = 0$) For this case, the momentum distribution has recently been computed ([19]; see also Ref. [34]), yet we plot it in Figure 5 for comparison. It evolves from a Gaussian $\tilde{\rho}(k)/2\pi = \pi^{-1/2}e^{-k^2}$ at $g = 0$ (with a maximum at $\tilde{\rho}(0) = .35\ldots$) to a slightly sharper peak, here depicted for $g = .4$. This squares with the broadened natural orbital ϕ_0 in that regime, as found in Sec. IV B 2. In the same light one sees that for $g = 4.7$, where fragmentation has set in, the peak at $k = 0$ is even more pronounced, while $\tilde{\rho}(k)$ has also developed a long-range tail. Both
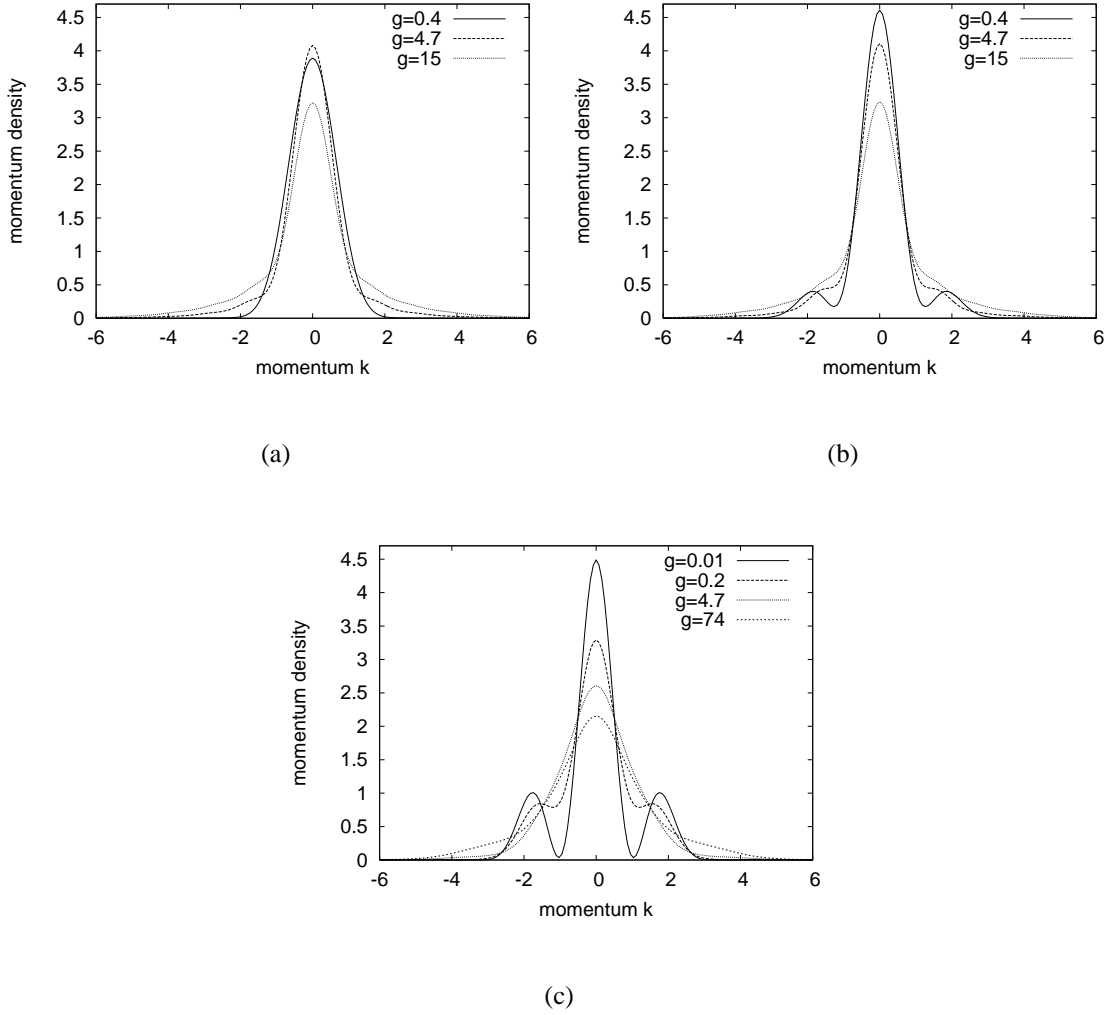
14

(a)

(b)

(c)

Figure 5: Momentum density $\tilde{\rho}(k)$ for (a-b) $N = 5$ bosons in a double-well trap of barrier height h. (left: $h = 0$, right: $h = 5$); shown are the interaction strengths $g = 0.4$, 4.7, 15. (c) The case $N = 4, h = 10$ for $g = 0.01$, 0.2, 4.7, 74.

observations are easily accounted for. The $k = 0$ behavior, for one thing, was argued to correspond to the off-diagonal long-range behavior of $\rho_1(x, x')$ in Sec. II B. This fits in with our observation that the off-diagonal range was indeed extended in that g-regime, as seen in Fig. 2.

The asymptotics $k \to \infty$ is in turn determined by the short-range interaction, which is known to culminate in the k^{-4} tail for $g \to \infty$. This latter consequence is in fact confirmed here (see $g = 15$). Moreover, notice that the $k = 0$ peak is bound to diminish. In other words, the momentum spectrum is redistributed toward higher k, in accordance with the reduction of off-diagonal long-range order. This fact stands in marked contrast to the homogeneous system, which in the Tonks-

15

Girardeau limit had an infrared divergence $\tilde{\rho}(k) = O(k^{-1/2})$. The seeming contradiction is owed to the fact that we deal with a bounded system, which cannot display true long-range order.

Double well (h = 5) The momentum spectrum for a double well looks quite different from the start ($g = 0.4$): it exhibits two sidelobes. This can be explained by the symmetric orbital $\phi_0(x) = c[\varphi(x - x_0) + \varphi(x + x_0)]$, which leads to a cosine-type modulation of $\tilde{\rho}$ due to $\hat{\phi}_0(k) = c\cos(kx_0)\hat{\varphi}(k)$. These sidelobes get even more distinct as $h \to \infty$ (see Fig. 5c). With increasing repulsion ($g = 4.7$), there are two competing effects. On the one hand, the orbitals are flattened a little, which should result in a slightly sharper momentum distribution. It turns out, though, that the effect of fragmentation outperforms the former one even for tiny interactions: admixing an anti-symmetric orbital ϕ_1 adds a $\sin(kx_0)$-type modulation, thus washing out the sidelobes as well as the central peak. Note that this effect is even more striking for $h = 10$, where it kicks in already for $g = 0.2$. In other words, the signature of the Gross-Pitaevskii regime in the harmonic trap—the initial sharpening of the $k = 0$ peak—is lost in the case of a sufficiently pronounced double well.

Along the lines of the remarks in the previous paragraph, we mention that the behavior for large correlations g is again universal as far as the k^{-4} tail for $k \to \infty$ is concerned. It also has a reduced peak for zero momentum, in accordance with the loss of long-range order found in Sec. IV A.

V. TWO-BODY CORRELATIONS AND DISCUSSION

The focal point of our discussion so far has been the one-particle density matrix, and related quantities. However useful they are in studying fragmentation, they are by construction ignorant of an essential ingredient: the two-body correlations, which have of course been traced out in the definition of ρ_1. Studying the (diagonal) two-particle density $\rho_2(x_1, x_2)$ may thus promise to yield an intriguing look behind the scenes of the one-particle picture. We will round off this section by commenting on the relation of our results to approximate methods such as multi-orbital mean-field theory and the two-mode model.

A. Two-particle correlations

For weak enough interactions, $g \to 0$, the system is in an uncorrelated state characterized by $\rho_2(x_1, x_2) = \rho(x_1)\rho(x_2)$. The first effect of the two-body interaction is to distort the one-particle density governed by the Gross-Pitaevskii eq., while from some point on ρ_2 will reflect
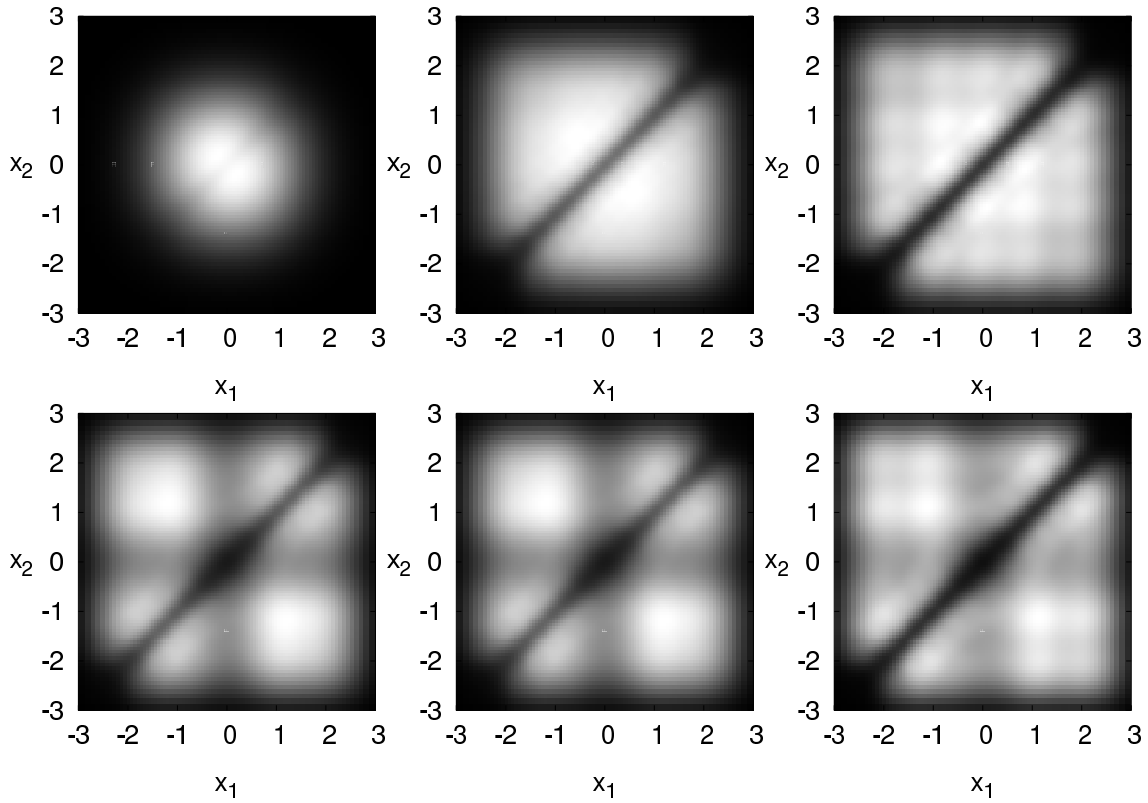
Figure 6: 2-particle density $\rho_2(x_1, x_2)$ for $N = 5$ bosons in a double-well trap of barrier height h. Top row: $h = 0$, bottom row: $h = 5$; shown are the interaction strengths $g = 0.4,\ 4.7,\ 10$ from left to right.

the correlations that are introduced by $V(x_i - x_j)$. As the pair-interaction energy is $\mathrm{tr}(V\rho_2) \overset{\sigma \to 0}{\sim}$ $g \int dx \rho_2(x, x)$, keeping it low amounts to depleting the 'correlation diagonal' $\{x_1 = x_2\}$.

For $g = 0.4$ (Fig. 6), a closer look reveals exactly that. In the case $h = 0$, a slight dip along the diagonal is formed as the density is being smeared out a little. In turn, for the double well ($h = 5$), the density is pumped into the off-diagonal peaks, which is indicative of a correlated state. Note that this 'dip' on the correlation diagonal is a feature of the two-body picture; in the one-particle density $\rho = \int dx_2 \rho_2(\cdot, x_2)$ it is smoothed out and thus much less visible. As g is increased ($g = 4.7$), we are in the regime of fragmentation. Here the wave function develops marked minima at points of collision, $x_i = x_j$, as exemplified for two atoms in a harmonic trap [13]. This carries over to ρ_2, where a characteristic correlation hole emerges, cutting the plot into halves. Despite that, the overall pattern still bares a resemblance to the non-interacting case. This changes when the system approaches fermionization, cf. $g = 10$. Here we encounter the simultaneous splitting into humps familiar from the one-particle density as presented in Ref. [20]. In this context, these wiggles signify that, if one boson resides at x_1, then any second one is likely

to be found at $N - 1$ distinct spots x_2, just not at $x_2 = x_1$. The exact distribution depends on the trap, of course. For $h = 0$, the checkerboard pattern is quite regular and has a larger amplitude about $x = 0$, while for $h = 5$ the peaks are in a way packed into either well but suppressed in the center.

B. Relation to approximation schemes

Let us stop to wrap up what we have found and work out the key points by contrasting them with two well-known approximations. The transition from a macroscopic state $\phi_0^{\otimes N}$ to a fermionized state follows different pathways for different traps. For a harmonic trap, the lowest orbital retains its singular importance for any interaction strength. In a double well, as the barrier height tends to infinity, the route passes through a configuration fairly well approximated by two single-particle states ϕ_a, i.e., a number state $|N/2, N/2\rangle$ (or generally a superposition of states $|n_0', n_1'\rangle$). For higher g, in turn, the system will be fermionized, and the first N single-particle orbitals will have dominant weights n_a.

The stopover near the fragmented state $|N/2, N/2\rangle$ in the double well is the essence of the commonplace *two-mode approximation* (see, e.g., [24]). It can be recovered in MCTDH by restricting the number of single-particle functions to $n = 2$ (see III), which sets the subspace to $\mathrm{span}\{|n_0', n_1'\rangle \mid \sum_a n_a' = N\}$. Needless to say, it becomes only exact in the limit $h \to \infty$ and $g \to 0^+$. Never is it able to describe anything but that coarse-grained fragmentation into two simple fragments, let alone the typical fermionization pattern in $\rho(x)$, the correlation hole evidenced in $\rho_2(x_1, x_2)$, or the short-range-driven k^{-4} tail evidenced in the momentum spectrum.

The simple two-mode state above, $|n_0', n_1'\rangle$, is contained in a general *multi-orbital mean-field* theory, which yields the variationally best number state [16, 35]. Among its most impressive successes has been a description of the evolution from the Gross-Pitaevskii regime to fermionization. The latter one was modeled by a state with $n_a' = 1$ $(a < N)$. We have pointed out [20] that this state emerges from our approach as a robust yet spurious solution if the Hilbert space is restricted to $\mathrm{span}\{\Phi_J \mid j_\kappa \leq N\}$. Also, we have argued that the number state gets all local quantities (the reduced densities as well as the energy) *about* right. By contrast, it is not designed to reproduce correlation-sensitive functions, such as the off-diagonal density matrix. Even though the use of several orbitals also serves to destroy off-diagonal long-range order (which hinges on the superposition of different orbitals, as delineated in II B), the incorrect populations (n_a) make
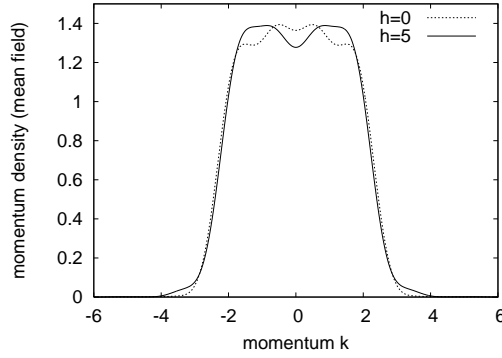
Figure 7: The spurious momentum density $\tilde{\rho}(k)$ as obtained within the restriction to $n = N = 4$ orbitals in the Tonks-Girardeau limit. Plotted are the results for the harmonic trap ($h = 0$) and the double well ($h = 5$) for large interactions g. The states correspond to number states $|1_0, \ldots, 1_{N-1}\rangle$.

for a *fermionic* rather than a *bosonic* momentum density, as displayed in Fig. 7. It resembles the spatial distribution and not the $k = 0$-peaked and long-range structure in Fig. 5. This reflects the fact that the mean-field approach cannot possibly recover the correct short-range behavior, which would require explicit correlations or, equivalently, the superposition of *several* single-particle configurations Φ_J. Instead it only mimics the spatial separation.

Lastly, one should be aware that for a state with $n_a = 1 \,\forall a$, the spectrum of ρ_1 is entirely degenerate; hence the eigenvectors ϕ_a are only defined up to unitary transform (U_{ab}). In this light they might as well be thought of as spatially localized, as opposed to distorted oscillator functions ($h = 0$) or anti-/symmetric orbitals ($h = 5$).

VI.   CONCLUSIONS AND OUTLOOK

The focus of this work have been correlation aspects of the numerically exact ground state of few atoms in different double-well traps. This way we have extended the more intuitive notion of the pathway from the weakly interacting regime via fragmentation to fermionization as described in our previous work [20]. On the other hand, this article closes the gap between the non-interacting and the Tonks-Girardeau limit, for which aspects such as off-diagonal long-range order and the momentum spectrum have been understood, and shows how these very different cases connect. Our method is based on the Multi-Configuration Time-Dependent Hartree code, whose efficient variational approach allows us to compute the ground state to a high accuracy.

As one key result, we have highlighted the relation of the fragmentation process to the diminishing of off-diagonal long-range order in the one-body density matrix. That mechanism has been explained in terms of the eigenvectors of the density matrix, the natural orbitals. These also allow us to relate the loss of long-range order to the momentum spectrum, whose markedly peaked structure in the non-interacting case is stretched into a characteristic high-momentum tail for stronger interactions. Moreover, we show how the populations of all natural orbitals evolve, which not only illuminates how the fragmentation mechanism is altered as the trap is turned from a harmonic one to a double well, but also casts a light on the validity of the two-mode model. Finally, we have laid out in more detail the two-body nature of the correlations, which reflects in the formation of a 'correlation hole' and culminates in the onset of the familiar checkerboard pattern. This goes well beyond the scope of approximation schemes inspired by a single-particle picture.

With these investigations, the analysis of the ground state of few-boson systems in double-well traps may be considered complete. Future extensions of these studies appear obvious. For one thing, the addition of more wells to the trap is of interest. This touches on the question of the few-body analog of an optical lattice, and its related effects such as the superfluid/Mott-insulator transition. On the other hand, a physically thrilling situation would involve not only the ground state, but also excitations, and eventually as well looking into the dynamics of the system. Given the richness of these fields on the many-atom level, the detailed study of few atoms promises a wide range of applications. All these efforts may serve as a bridge toward a better control of ultracold few-body systems.

[1] L. Pitaevskii and S. Stringari, *Bose-Einstein Condensation* (Oxford University Press, Oxford, 2003).

[2] F. Dalfovo, S. Giorgini, L. Pitaevskii, and S. Stringari, Rev. Mod. Phys. **71**, 463 (1999).

[3] C. J. Pethick and H. Smith, *Bose-Einstein condensation in dilute gases* (Cambridge University Press, Cambridge, 2001).

[4] A. J. Leggett, Rev. Mod. Phys. **73**, 307 (2001).

[5] M. Olshanii, Phys. Rev. Lett. **81**, 938 (1998).

[6] M. Girardeau, J. Math. Phys. **1**, 516 (1960).

[7] H. G. Vaidya and C. A. Tracy, Phys. Rev. Lett. **42**, 3 (1979).

[8] A. Minguzzi, P. Vignolo, and M. P. Tosi, Phys. Lett. A **294**, 222 (2002).

[9] T. Kinoshita, T. Wenger, and D. S. Weiss, Science **305**, 1125 (2004).

[10] B. Paredes *et al.*, Nature **429**, 277 (2004).

[11] M. Girardeau, E. M. Wright, and J. M. Triscari, Phys. Rev. A **63**, 033601 (2001).

[12] T. Papenbrock, Phys. Rev. A **67**, 041601 (2003).

[13] M. A. Cirone, K. Góral, K. Rzazewski, and M. Wilkens, J. Phys. B **34**, 4571 (2001).

[14] Y. Hao, Y. Zhang, J. Q. Liang, and S. Chen, Phys. Rev. A **73**, 063617 (2006).

[15] K. Sakmann, A. I. Streltsov, O. E. Alon, and L. S. Cederbaum, Phys. Rev. A **72**, 033613 (2005).

[16] O. E. Alon and L. S. Cederbaum, Phys. Rev. Lett. **95**, 140402 (2005).

[17] D. Masiello, S. B. McKagan, and W. P. Reinhardt, Phys. Rev. A **72**, 063624 (2005).

[18] A. I. Streltsov, O. E. Alon, and L. S. Cederbaum, Phys. Rev. A **73**, 063626 (2006).

[19] F. Deuretzbacher, K. Bongs, K. Sengstock, and D. Pfannkuche, cond-mat/0604673 (2006).

[20] S. Zöllner, H.-D. Meyer, and P. Schmelcher, quant-ph/0605210 (2006).

[21] H.-D. Meyer and G. A. Worth, Theor. Chem. Acc. **109**, 251 (2003).

[22] H.-D. Meyer, in *The Encyclopedia of Computational Chemistry*, edited by P. v. R. Schleyer *et al.* (John Wiley and Sons, Chichester, 1998), Vol. 5, pp. 3011–3018.

[23] M. H. Beck, A. Jäckle, G. A. Worth, and H.-D. Meyer, Phys. Rep. **324**, 1 (2000).

[24] R. W. Spekkens and J. E. Sipe, Phys. Rev. A **59**, 3868 (1999).

[25] O. Penrose and L. Onsager, Phys. Rev. **104**, 576 (1956).

[26] E. H. Lieb, R. Seiringer, and J. Yngvason, Phys. Rev. Lett. **91**, 150401 (2003).

[27] C. N. Yang, Rev. Mod. Phys. **34**, 694 (1962).

[28] V. I. Yukalov and M. D. Girardeau, cond-mat/0507409 (2005).

[29] H.-D. Meyer, U. Manthe, and L. S. Cederbaum, Chem. Phys. Lett. **165**, 73 (1990).

[30] G. A. Worth, M. H. Beck, A. Jäckle, and H.-D. Meyer, The MCTDH Package, Version 8.2, (2000). H.-D. Meyer, Version 8.3 (2002). See http://www.pci.uni-heidelberg.de/tc/usr/mctdh/.

[31] R. Kosloff and H. Tal-Ezer, Chem. Phys. Lett. **127**, 223 (1986).

[32] H.-D. Meyer, F. L. Quéré, C. Léonard, and F. Gatti, Chem. Phys. in press (2006).

[33] J. C. Light, I. P. Hamilton, and J. V. Lill, J. Chem. Phys. **82**, 1400 (1985).

[34] G. E. Astrakharchik and S. Giorgini, Phys. Rev. A **68**, 031602 (2003).

[35] L. S. Cederbaum and A. I. Streltsov, Phys. Lett. A **318**, 564 (2003).